7th International Symposium on Three-Dimensional Electromagnetics
Vancouver, BC, Canada, November 13–15, 2023

# On the Robustness, Efficiency and Scalability of an Iterative Framework in Combination With the Block-Based PREconditioner For Square Blocks PRESB Applied To Controlled-Source Electromagnetic Modelling

Michael Weiss[1], Thomas Kalscheuer[2] and Maya Neytcheva[2]
[1]Leibniz Institute for Applied Geophysics, Hanover, Germany
[2] Uppsala University, Uppsala, Sweden

## Summary

We introduce an efficient and robust iterative framework based on the Block-Based PREconditioner for Square Blocks known as PRESB for 3D controlled-source electromagnetic problems in frequency domain. We study the robustness, efficiency and scalability of the iterative solver and compare it to other solution methods.

**Keywords:** iterative solution methods, preconditioning, numerical modelling, controlled-source electromagnetics

## Introduction

Electromagnetic (EM) surveys may comprise numerous receivers and multiple sources in complex three-dimensional (3D) settings with topography and subsurface structures. Accurate numerical forward or inverse modelling of such large-scale studies accounting for their respective survey setup as well as reliefs requires large 3D meshes which may yield computational models of large proportion ranging from a couple to hundreds of millions degrees of freedom. Solving problems of these sizes is computationally challenging and expensive and consequently strategies reducing the computational burden are paramount. A key component of both the forward and inverse problem is the solution of the algebraic system of equations stemming from Maxwell's equations, that is solving a discrete system of the form $\mathbf{Ux} = \mathbf{b}$ where matrix $\mathbf{U}$ is sparse and non-singular and where $\mathbf{x}$ and $\mathbf{b}$ denote the solution and source vectors, respectively.

In general, two types of numerical solution methods are employed to obtain solutions of linear systems of equations, namely direct and iterative approaches with their respective advantages and disadvantages. Direct methods find broad application due to their generality, robustness and ease of use and despite their high memory requirements (proportional to $\mathcal{O}(N^2)$ in 3D with $N$ denoting the number of degrees of freedom) for large problems. Iterative solution techniques on the other hand are considered very resource friendly, but may be afflicted by slow convergence or even divergence if applied without adequate and problem-specific preconditioning techniques as preconditioning greatly improves the robustness and efficiency of iterative methods.

The objective of this work is to present a developed and efficient iterative solution framework for controlled-source EM problems. The framework is shown to be robust to discretisation and material parameters. In addition, the framework is compared against other iterative and direct solution methods. Lastly, the scalability of the framework is investigated and studied.

## Method

The algebraic linear system of equations governing the physics encountered in frequency-domain controlled-source EM problems based on a total field formulation is given by

$$(\mathbf{K} + i\mathbf{M}_\sigma - \mathbf{M}_\varepsilon)\,\mathbf{e} = \mathbf{b}, \tag{1}$$

where matrix $\mathbf{K}$ denotes the sparse symmetric positive semi-definite stiffness matrix, matrices $\mathbf{M}_\sigma$ and $\mathbf{M}_\varepsilon$ are the sparse symmetric positive definite mass matrices. The vectors $\mathbf{e}$ and $\mathbf{b}$ denote the solution vector and the right hand side vector.
This sparse symmetric complex-valued system can be cast into an equivalent real-valued two-by-two block system that reads as follows

$$\underbrace{\begin{bmatrix} \mathbf{M}_\sigma & -(\mathbf{K} - \mathbf{M}_\varepsilon) \\ \mathbf{K} - \mathbf{M}_\varepsilon & \mathbf{M}_\sigma \end{bmatrix}}_{\mathbf{C_{RI}}} \begin{bmatrix} \mathbf{e_R} \\ -\mathbf{e_I} \end{bmatrix} = \begin{bmatrix} \mathbf{b_I} \\ \mathbf{b_R} \end{bmatrix}, \tag{2}$$

and belongs to systems of the more general type of form

$$\boldsymbol{\mathcal{A}} = \begin{bmatrix} \mathbf{A} & -b\,\mathbf{B_2} \\ a\,\mathbf{B_1} & \mathbf{A} \end{bmatrix}. \tag{3}$$

For systems of this type and if matrix $\mathbf{A}$ is symmetric positive definite and the non-zero scalars $a$ and $b$ are of the same sign, there exists an efficient preconditioner known as PRESB short for 'PREconditioner for Square Blocks' (see e.g. Axelsson et al., 2014) that is of form

$$\boldsymbol{\mathcal{P}}_{\text{PRESB}} = \begin{bmatrix} \mathbf{A} & -b\,\mathbf{B}_2 \\ a\,\mathbf{B_1} & \mathbf{A} + \sqrt{ab}(\mathbf{B_1} + \mathbf{B_2}) \end{bmatrix} \tag{4}$$

and for which it can be shown that all the eigenvalues of the preconditioned system $\boldsymbol{\mathcal{P}}_{\text{PRESB}}^{-1}\boldsymbol{\mathcal{A}}$ lie in the interval 0.5 and 1 (see e.g. Axelsson et al., 2016). The clustering of the eigenvalues translates to excellent convergence properties of the preconditioner. In addition, the preconditioner is robust with respect to mesh discretisation and material parameters. The preconditioner possesses the following block factorisation

$$\begin{bmatrix} \mathbf{A} & -\mathbf{B}^T \\ \mathbf{B} & \mathbf{A} + \mathbf{B} + \mathbf{B}^T \end{bmatrix} = \begin{bmatrix} \mathbf{I} & -\mathbf{I} \\ \mathbf{0} & \mathbf{I} \end{bmatrix} \begin{bmatrix} \mathbf{A} + \mathbf{B} & \mathbf{0} \\ \mathbf{0} & \mathbf{I} \end{bmatrix} \begin{bmatrix} \mathbf{I} & \mathbf{0} \\ \mathbf{B} & \mathbf{I} \end{bmatrix} \begin{bmatrix} \mathbf{I} & \mathbf{0} \\ \mathbf{0} & \mathbf{A} + \mathbf{B}^T \end{bmatrix} \begin{bmatrix} \mathbf{I} & \mathbf{I} \\ \mathbf{0} & \mathbf{I} \end{bmatrix}. \tag{5}$$

Applied to the two-by-two system (2), the computational cost of applying the PRESB preconditioner amounts to solving to linear systems with $\mathbf{M}_\sigma + (\mathbf{K} - \mathbf{M}_\varepsilon)$ and $\mathbf{M}_\sigma + (\mathbf{K} - \mathbf{M}_\varepsilon)^T$, one multiplication with the matrix $\mathbf{M}_\sigma$ and three vector additions. This is equivalent to solving a system of the form

$$\underbrace{\begin{bmatrix} \mathbf{M}_\sigma & -(\mathbf{K} - \mathbf{M}_\varepsilon) \\ \mathbf{K} - \mathbf{M}_\varepsilon & \mathbf{M}_\sigma + 2(\mathbf{K} - \mathbf{M}_\varepsilon) \end{bmatrix}}_{\mathbf{P}_{\text{PRESB}}} \begin{bmatrix} \mathbf{w_1} \\ \mathbf{w_2} \end{bmatrix} = \begin{bmatrix} \mathbf{f_1} \\ \mathbf{f_2} \end{bmatrix}, \tag{6}$$

which is summarised in Algorithm 1 as

**Algorithm 1:** Solving linear system with preconditioner $\mathbf{P}_{\text{PRESB}}$

Solve $(\mathbf{M}_\sigma + \mathbf{K} - \mathbf{M}_\varepsilon)\,\mathbf{g} = \mathbf{f_1} + \mathbf{f_2}$
Compute $\mathbf{M}_\sigma\mathbf{g}$ and $\mathbf{f_1} - \mathbf{M}_\sigma\mathbf{g}$
Solve $(\mathbf{M}_\sigma + \mathbf{K} - \mathbf{M}_\varepsilon)\,\mathbf{h} = \mathbf{f_1} - \mathbf{M}_\sigma\mathbf{g}$
Compute $\mathbf{w_1} = \mathbf{g} + \mathbf{h}$ and $\mathbf{w_2} = -\mathbf{h}$

The linear systems in the above procedure constitute discretised $\mathcal{H}_0(\text{curl}, \Omega)$ problems which can be solved fast and efficiently using the auxiliary-space technique (see e.g. Xu, 1996; Hiptmair & Xu, 2007; Kolev & Vassilevski, 2009). Here, the auxiliary-space Maxwell solver (AMS) implemented in hypre (Falgout & Yang, 2002) is used to precondition a generalised conjugate residual method (GCR; Eisenstat et al., 1983) to obtain solution to systems involving $(\mathbf{M}_\sigma + \mathbf{K} - \mathbf{M}_\varepsilon)$. Alternatively, the systems at hand can be solved using a direct solver such as MUMPS (Amestoy et al., 2000) for example.

The two-by-two system given in equation (2) is solved using a GCR method and preconditioned with PRESB and the iterative solver is described in Algorithm 2. The algorithm thus consists of an outer solver with a nested inner solver. Each outer iteration requires applying the preconditioner PRESB thus necessitating two inner solves as outlined in Algorithm 1.

**Algorithm 2:** PRESB-preconditioned GCR method

**Input:** $\mathbf{C_{RI}}, \mathbf{b_{R,I}}, \mathbf{M}_\sigma + \mathbf{K} - \mathbf{M}_\varepsilon, \mathbf{M}_\sigma$, initial guess $\mathbf{x}_0$, tol
**Output:** $\mathbf{e_{R,I}}$
Set $\mathbf{r}_0 = \mathbf{b} - \mathbf{C_{RI}}\mathbf{x}_0$
**for** $i = 0, \ldots m$ **do**
  Solve $\mathbf{P}_{PRESB}\mathbf{p}_i = \mathbf{r_i}$ using Algorithm 1
  $\mathbf{q}_i = \mathbf{C_{RI}}\mathbf{p}_i$
  $\mathbf{q}_i = \mathbf{q}_i - \sum_{j=0}^{i-1} \mathbf{q}_j \frac{(\mathbf{q}_i, \mathbf{q}_j)}{(\mathbf{q}_j, \mathbf{q}_j)}$
  $\mathbf{p}_i = \mathbf{p}_i - \sum_{j=0}^{i-1} \mathbf{p}_j \frac{(\mathbf{q}_i, \mathbf{q}_j)}{(\mathbf{q}_j, \mathbf{q}_j)}$
  $\alpha_i = \frac{(\mathbf{r}_i, \mathbf{q}_i)}{(\mathbf{q}_i, \mathbf{q}_i)}$
  $\mathbf{x}_{i+1} = \mathbf{x}_i + \alpha_i\mathbf{p}_i$
  $\mathbf{r}_{i+1} = \mathbf{r}_i - \alpha_i\mathbf{q}_i$
  **if** $\frac{||\mathbf{r}_{i+1}||_2}{||\mathbf{r}_0||_2} < tol$ **then** $\mathbf{e_{R,I}} = \mathbf{x}_{i+1}$ & Stop
**end**

The iterative framework described has been implemented using distributed-memory parallelism and makes use of functionalities provided by the open-source libraries PETSc (Balay et al., 2022), hypre (Falgout et al., 2006) and MUMPS (Amestoy et al., 2000) as a standalone Fortran code (see Weiss et al., 2023). More recently, the iterative framework has been added to custEM (Rochlitz et al., 2019) and will be made available with the next version update.

## Results

### Robustness

The results presented in the following subsection summarise the findings in Weiss et al. (2023). For the reader's convenience, the essential information and observations are repeated here.

The robustness of the iterative framework is tested

using two problems as depicted in Figure 1. Table 1 indicates relevant information about the model and source for Problems 1 and 2.
All simulations presented are run using two MPI processes on a AMD Ryzen Thread-ripper 2950X 16-core processor with a clock frequency of 3.5 GHz and with 128 GB RAM. Moreover, each computation is stopped when the relative residuals of the outer and inner solver dips below $10^{-12}$ and $10^{-3}$, respectively.

The iterative framework is tested for Problem 1 with respect to variable frequencies as well as problem size at the same time. Table 2 displays the outer iteration counts and simulation times for three problem sizes and for four frequencies spanning almost five orders of magnitude. It can readily been observed that the outer iteration count is very stable across the tested range of frequencies. In addition, the outer iteration count is independent of the problem size.

Problem 2 is used to asses the robustness of the iterative solver with respect to magnetic permeability and dielectric permittivity. Results of simulations for the chosen material properties (see Table 1) are given in Table 3 and verify that the iterative framework is robust with regard to variable material properties as indicated by the outer iteration counts.

### Comparison and Scalability

The iterative solver is compared to other solution methods and tested with regard to scalability using the crooked loop example on a three-layer Earth from the custEM toolbox (Rochlitz et al., 2019). All simulations are run using polynomial of first order on the example's finest mesh yielding $13'447'978$ degrees of freedom for the two-by-two system. The iterative procedure is terminated when the relative residual of the outer algorithm falls below $10^{-8}$. All computations times are obtain on a Dell PowerEdge R940 server with four Intel Xeon Gold 6154 processors clocked at 3 GHz and 48 LRDIMM 64 GB, DDR4-2666, Quad Ranks.

The preconditioner PRESB is compared to a highly efficient block diagonal preconditioner (see e.g. Chen et al., 2010; Grayver & Bürg, 2014). The numerical experiments for this comparison are run using 56 MPI processes. Figure 2 shows the convergence histories for simulations using the PRESB and block diagonal preconditioner, respectively, across four frequencies. In addition, the corresponding simulation times are annotated in the plots. It is evident that PRESB requires fewer iterations to reach the desired relative residual and thus saves some time compared to the block diagonal preconditioner.

The scalability, time and memory requirements for the direct solver MUMPS and the iterative framework are compared in Figure 3. The plot on the left displays the run times against the number of parallel processes used and indicates that the iterative framework reduces the simulation times by a factor of 2.9 to 3.8. On the right, the memory usage is tracked over the run time for both the direct solver (blue) and iterative algorithm (red). Peak memory consumption is annotated in the plot. Overall, the iterative framework requires approximately one order of magnitude less memory for this example with a system size of $13'447'978$ than the direct solver MUMPS.

All in all, the developed iterative framework proves highly efficient in terms of computational time and memory requirements in comparison to the direct solver MUMPS. Further, as indicated by the convergence histories and the simulations times in Figure 2, PRESB is slightly more efficient than the block diagonal preconditioner. As the implementation of both preconditioners is based on similar building blocks, changing to the preconditioner PRESB is straight forward and simple and thus suggested.

Figure 3 further reveals the considerable potential of the algorithm in terms of computational resources which may be harnessed in inverse modelling by incorporating the iterative solver as an underlying engine for it.

## Conclusion

The numerical experiments attest to the robustness of the PRESB-preconditioned GCR method with regard to frequency, problem size, mesh discretisation and spatially variable material properties, that is electric conductivity, magnetic permeability and dielectric permittivity. Comparisons with other solvers and the scalability example demonstrate the potential of the iterative solver in terms of computational resources and as a possible future engine for inversions.

## Acknowledgements

This work was partly funded by Uppsala's Center for Interdisciplinary Mathematics (CIM) and by the Germany Ministry for Education and Research (BMBF) as part of the DESMEX II project in the framework of the research and development program Fona-r4 under grant 033R130DN.

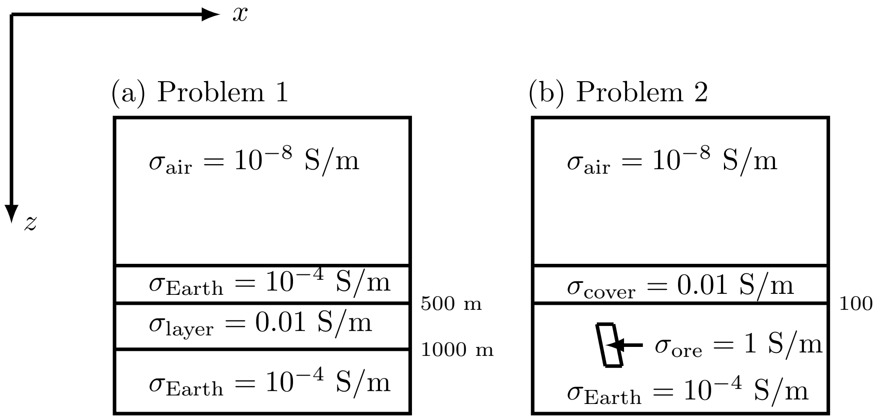


**Figure 1:** Schematic profile of Problems 1 and 2 (see Weiss et al., 2023).

**Table 1:** Model information for Problems 1 and 2

| Model | Problem 1 - Layered Earth | Problem 2 - 3D model |
|---|---|---|
| Domain size [km$^3$] | $30 \times 30 \times 30$ | $30 \times 36 \times 30$ |
| Coordinates of 3D body | - | $(-4000, 2000, \pm 331), (-3000, 2000, \pm 331)$ $(-3000, 5000, \pm 331), (-2000, 5000, \pm 331)$ |
| Source type | Grounded cable extending from $(-100, 0, 0)$ m to $(100, 0, 0)$ m | Grounded cable extending from $(-75, 0, 0)$ m to $(59, 0, 0)$ m |
| Source moment [Am] | 100 | 100 |
| Conductivities [S/m] | $\sigma_{\text{air}} = 10^{-8}$, $\sigma_{\text{Earth}} = 10^{-4}$, $\sigma_{\text{layer}} = 10^{-2}$ | $\sigma_{\text{air}} = 10^{-8}$, $\sigma_{\text{Earth}} = 10^{-4}$, $\sigma_{\text{cover}} = 0.01$, $\sigma_{\text{ore}} = 1$ |
| Relative permeabilities | $\mu_{\text{air}} = 1$, $\mu_{\text{Earth}} = 1$, $\mu_{\text{layer}} = 1$ | $\mu_{\text{air}} = 1$, $\mu_{\text{Earth}} = 1$, $\mu_{\text{cover}} = 1$, $\mu_{\text{ore}} = 1$ or 10 |
| Relative permittivities | $\varepsilon_{\text{air}} = 1$, $\varepsilon_{\text{Earth}} = 1$, $\varepsilon_{\text{layer}} = 1$ | $\varepsilon_{\text{air}} = 1$, $\varepsilon_{\text{Earth}} = 5$, $\varepsilon_{\text{cover}} = 20$, $\varepsilon_{\text{ore}} = 1$ |
| Approximation order | 1st | 1st |
| # elements | $54 \times 54 \times 54$ | 332'580 |
| # degrees of freedom | 980'100 | 2'033'986 |

**Table 2:** Problem 1: Robustness with respect to problem size and across frequency for the iterative solver shown by the outer iteration counts ($N_{\text{it}}^{\text{outer}}$) and solving times (time [s]) (see Weiss et al., 2023).

| | frequency [Hz] | | | | | | | |
|---|---|---|---|---|---|---|---|---|
| | 0.1 | | 10 | | 1000 | | 8000 | |
| Problem size | $N_{\text{it}}^{\text{outer}}$ | time [s] | $N_{\text{it}}^{\text{outer}}$ | time [s] | $N_{\text{it}}^{\text{outer}}$ | time [s] | $N_{\text{it}}^{\text{outer}}$ | time [s] |
| 980'100 | 7 | 42.2 | 16 | 79.3 | 19 | 70.2 | 18 | 96.8 |
| 3'641'400 | 8 | 152.9 | 15 | 286.4 | 18 | 272.6 | 19 | 310.2 |
| 6'879'600 | 8 | 343.4 | 16 | 646.5 | 18 | 521.8 | 18 | 790.5 |

**Table 3:** Problem 2: Robustness with regard to spatially variable dielectric permittivity and for two different magnetic permeabilities for the ore body across frequencies for the iterative algorithm shown by the outer iteration counts ($N_{it}^{outer}$) and solution times (time [s]) (see Weiss et al., 2023).

| relative dielectric permittivity of air, cover, host rock and ore body | $\varepsilon_r^{air} = 1$, $\varepsilon_r^{cover} = 20$, $\varepsilon_r^{Earth} = 5$, $\varepsilon_r^{ore\ body} = 1$ | | | |
|---|---|---|---|---|
| relative magnetic permeability of ore body | $\mu_r = 1$ | | $\mu_r = 10$ | |
| frequency [Hz] | $N_{it}^{outer}$ | time [s] | $N_{it}^{outer}$ | time [s] |
| 0.1 | 9 | 590.4 | 11 | 691.6 |
| 10 | 16 | 282.3 | 16 | 279.8 |
| 100 | 23 | 278.5 | 24 | 285.1 |
| 8000 | 18 | 341.0 | 18 | 322.4 |

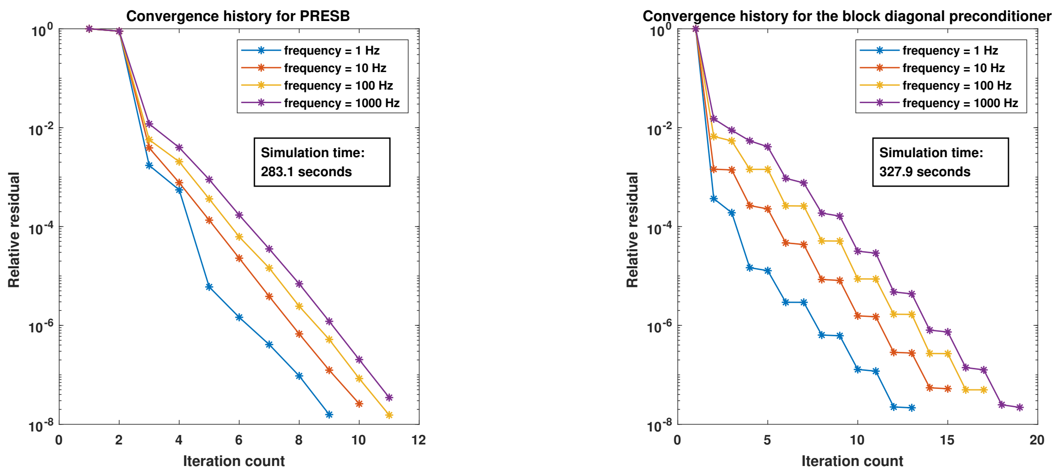


**Figure 2:** Comparison of the convergence histories for the crooked loop example run across four frequencies between PRESB and the block diagonal preconditioner. The subplots indicate the overall simulation time.

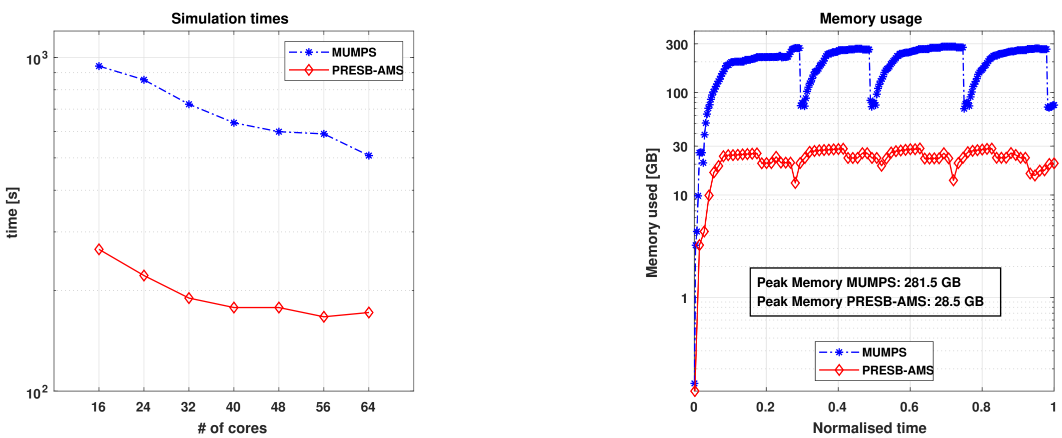


**Figure 3:** Scalabilities and computational requirements (time and memory) for the iterative framework denoted as PRESB-AMS and the direct solver MUMPS for the crooked loop example.

## REFERENCES


Amestoy, P. R., Duff, I. S., & L'excellent, J.-Y. (2000). Multifrontal parallel distributed symmetric and unsymmetric solvers. *Computer Methods in Applied Mechanics and Engineering*, *184*(2-4), 501–520.

Axelsson, O., Farouq, S., & Neytcheva, M. (2016). Comparison of preconditioned Krylov subspace iteration methods for PDE-constrained optimization problems. *Numerical Algorithms*, *73*(3), 631–663.

Axelsson, O., Neytcheva, M., & Ahmad, B. (2014). A comparison of iterative methods to solve complex valued linear algebraic systems. *Numerical Algorithms*, *66*(4), 811–841.

Balay, S., Abhyankar, S., Adams, M. F., Benson, S., Brown, J., Brune, P., et al. (2022). *PETSc/TAO users manual* (Tech. Rep. No. ANL-21/39 - Revision 3.17). Argonne National Laboratory.

Chen, J., Chen, Z., Cui, T., & Zhang, L.-B. (2010). An adaptive finite element method for the eddy current model with circuit/field couplings. *SIAM Journal on Scientific Computing*, *32*(2), 1020–1042.

Eisenstat, S. C., Elman, H. C., & Schultz, M. H. (1983). Variational iterative methods for nonsymmetric systems of linear equations. *SIAM Journal on Numerical Analysis*, *20*(2), 345–357.

Falgout, R. D., Jones, J. E., & Yang, U. M. (2006). The design and implementation of hypre, a library of parallel high performance preconditioners. In *Numerical Solution of Partial Differential Equations on Parallel Computers* (pp. 267–294). Springer.

Falgout, R. D., & Yang, U. M. (2002). hypre: A library of high performance preconditioners. In *International Conference on Computational Science* (pp. 632–641).

Grayver, A. V., & Bürg, M. (2014). Robust and scalable 3-D geo-electromagnetic modelling approach using the finite element method. *Geophysical Journal International*, *198*(1), 110–125.

Hiptmair, R., & Xu, J. (2007). Nodal auxiliary space preconditioning in H (curl) and H (div) spaces. *SIAM Journal on Numerical Analysis*, *45*(6), 2483–2509.

Kolev, T. V., & Vassilevski, P. S. (2009). Parallel auxiliary space AMG for H (curl) problems. *Journal of Computational Mathematics*, 604–623.

Rochlitz, R., Skibbe, N., & Günther, T. (2019). custEM: Customizable finite-element simulation of complex controlled-source electromagnetic data. *Geophysics*, *84*(2), F17–F33.

Weiss, M., Neytcheva, M., & Kalscheuer, T. (2023). Iterative solution methods for 3D controlled-source electromagnetic forward modelling of geophysical exploration scenarios. *Computational Geosciences*, *27*, 81–102.

Xu, J. (1996). The auxiliary space method and optimal multigrid preconditioning techniques for unstructured grids. *Computing*, *56*(3), 215–235.